lution (yield 4% based on the starting nickel ions). The electronic absorption and circular dichroism spectra of the complex in methanol are given in Figure 1. We have already reported that when a primary diamine, en or tn, is used, the structural features of nickel(II) complexes containing monosaccharides are evident in CD spectra.[4,6,7] That is to say, the CD curves of the D-glucose and D-mannose complexes are nearly mirror images of the corresponding CD curves in the first absorption region. However, in this study, the CD curve of **8** is not a mirror image of but is similar to the CD curve of the complex Man1(Cl) (**6**). HPLC analysis shows that the ratio of monosaccharide to nickel ion in **8** is 2.8:2.0, suggesting a binuclear complex. Further, of the monosaccharides recovered from the complex, 28% are D-glucose and 72% are surprisingly D-mannose, indicating that the starting D-glucose was partially epimerized during the reaction. From these results, it is assumed that **8** is the mixture of the binuclear complexes having the structure of mannofuranoside bridging (Figure 6). This observation is very important in relation to the transformation of sugars by metal complexes and, in fact, gave us a significant clue to develop the C-2 epimerization of aldoses promoted by nickel(II)-diamine complexes.[27]

Acknowledgment. The authors wish to thank Professors Kozo Sone and Yutaka Fukuda of Ochanomizu University for obtaining magnetic data and for their helpful suggestions. They also thank the Ministry of Education for a Grant-in-Aid (60470084).

Supplementary Material Available: Listings of anisotropic thermal parameters (Table IIb), atomic parameters of hydrogen atoms (Table IIc), torsional angles (Table VI), least-squares-plane data (Table VII), and bond distances and bond angles and a stereoscopic view of the unit cell (Figure 5) (10 pages); a table of structure factor amplitudes (11 pages). Ordering information is given on any current masthead page.

(27) (a) Tanase, T.; Shimizu, F.; Yano, S.; Yoshikawa, S. *J. Chem. Soc., Chem. Commun.* **1986**, 1001-1003. (b) Tanase, T.; Shimizu, F.; Kuse, M.; Yano, S.; Hidai, M.; Yoshikawa, S. *J. Chem. Soc., Chem. Commun.* **1987**, 659-661.

Contribution from the Departments of Molecular Biophysics and Biochemistry and Diagnostic Radiology, Yale University School of Medicine, New Haven, Connecticut 06510

Equilibrium and Kinetic Analysis of the Interaction of Mercury(II) with Cadmium(II) Metallothionein

Bruce A. Johnson and Ian M. Armitage*

Received January 25, 1987

The reaction of Cd-metallothionein (MT) with mercury(II) has been studied. The Cd_7-MT was titrated with from 1 to 14 equiv of $HgCl_2$, following which the cadmium(II) and mercury(II) contents, the partition coefficient on a size-exclusion HPLC column, and the UV spectra were measured. The results showed that mercury(II) quantitatively displaces cadmium(II) from the protein. An analysis of the UV spectral data by the method of singular value decomposition (SVD) was used to determine the number of spectrally distinct components and their fractional abundance throughout the titration. A minimum of three spectrally distinct components were found by this method; they corresponded to tetrahedral Cd-S, tetrahedral Hg-S, and linear Hg-S coordination geometries. Initially the mercury(II) occupies tetrahedral sites; however, above a Hg/MT stoichiometry of 4, there is a shift to linear coordination. The size-exclusion data indicate a shift to a more compact structure upon addition of mercury(II) to the metallothionein. Finally, the analysis of a UV spectrum of a mixture of the all-cadmium(II) and the all-mercury(II) metallothioneins indicates that the two forms undergo facile interprotein metal ion exchanges. The analysis of the kinetics of this reaction is best fit by second-order kinetics, which would be consistent with a mechanism whereby there was a direct interaction between the two MTs.

Introduction

Metallothioneins (MTs) are a unique class of low-molecular-weight proteins that are characterized by a high content of cysteine and a capacity to bind multiple moles of heavy metal ions.[1-3] MTs are nearly ubiquitous in nature, occurring in organisms ranging from fungi (*Neurospora* and *Saccharomyces*) to the mammals. While the physiological functions of MT have not been clearly defined as yet, it has been postulated to function both in providing a protective mechanism against an overload of toxic heavy metal ions such as cadmium and mercury and in maintaining a homeostasis of the essential metal ions, zinc and copper.[4]

Extensive use has been made of both chemical and optical spectroscopic techniques to characterize the nature of the MT metal binding sites and their relative affinities for different metal ions.[5,6] While these studies clearly show all 20 cysteine sulfurs in the mammalian MTs to be involved in metal ligation, the most explicit details about the metal ion-ligand coordination number and geometry were first revealed by ^{113}Cd NMR studies.[7] For the ^{113}Cd derivatives of rabbit liver MT, these studies indicate that the cadmium(II) ions are bound in two clusters consisting of four and three metals each, with the metal tetrahedrally coordinated to 11 and 9 cysteines, respectively. Recently, the structure of this protein has been more completely defined by both X-ray crystallography[8] and two-dimensional ^1H and ^1H-^{113}Cd NMR spectroscopy.[9] While these two studies differ in their assignment of specific cysteine residues to specific metal ions in the structure and hence differ in the predicted folding of the polypeptide chain, they both confirm the essential arrangement of bridging and terminal cysteine-metal ligands elucidated by the earlier ^{113}Cd NMR studies.

In comparison to the progress that has been made in the detailed structural elucidation of the cadmium(II) and cadmium(II)-

* To whom correspondence should be addressed at the Department of Molecular Biophysics and Biochemistry.

(1) Margoshes, M.; Vallee, B. L. *J. Am. Chem. Soc.* **1957**, *79*, 4813-4814.
(2) Dalgarno, D. C.; Armitage, I. M. In *Advances in Inorganic Biochemistry*; Vol. 6, Eichhorn, G. L., Marzilli, L., Eds.; Elsevier North-Holland: Amsterdam, 1984; Vol. 6, pp 113-138.
(3) Kägi, J. H. R., Kojima, Y., Eds. *Metallothionein. Proceedings of the Second International Meeting on Metallothionein and Other Low Molecular Weight Metal-Binding Proteins*; Birkhäuser: Basel, Switzerland, 1986.
(4) Petering, D. H.; Fowler, B. A. *EHP, Environ. Health Perspect.* **1986**, *65*, 217-224.
(5) Vasak, M.; Kägi, J. H. R. In *Metal Ions in Biological Systems*; Sigel, H., Ed.; Marcel Dekker: New York, 1983; Vol. 15, Chapter 6.
(6) Kägi, J. H. R.; Vasak, M.; Lerch, K.; Gilg, D. E. O.; Hunziker, P.; Bernhard, W.; Good, M. *EHP, Environ. Health Perspect.* **1984**, *54*, 93-103.
(7) Otvos, J. D.; Armitage, I. M. *Proc. Natl. Acad. Sci. U.S.A.* **1980**, *77*, 7094-7098.
(8) Furey, W. F.; Robbins, A. H.; Clancy, L. L.; Winge, D. R.; Wang, B. C.; Stout, C. D. *Science (Washington, D.C.)* **1986**, *231*, 704-710.
(9) (a) Braun, W.; Wagner, G.; Wörgörter, E.; Vasak, M.; Kägi, J. H. R.; Wüthrich, K. *J. Mol. Biol.* **1986**, *187*, 125-129. (b) Wagner, G.; Neuhaus, D.; Worgotter, E.; Vasak, M.; Kägi, J. H. R.; Wüthrich, K. *J. Mol. Biol.* **1986**, *187*, 131-135.

0020-1669/87/1326-3139$01.50/0

zinc(II) forms of the protein, relatively little is known about the structure, metal to ligand coordination number, and geometry in other metal derivatives of MT. Of the latter, the complex of MT with mercury(II) is of particular interest for the following reasons. First, as with cadmium(II) and zinc(II), exposure to mercury(II) both in vivo and in the cell culture leads to the increased formation of Hg–MT.[10-16] While this may occur in part by displacement of zinc(II) and cadmium(II) initially bound to MT, there are a number of studies which demonstrate that MT mRNA synthesis is also induced by mercury(II).[17,18] Secondly, ^{199}Hg is a spin-$^1/_2$ nucleus and thus offers the potential for the use of high-resolution NMR methods[19,20] in the detailed structural elucidation of this form of the protein in much the same way as was done with the ^{113}Cd MT derivatives. Inconsistencies in the reported in vitro procedures for preparing the Hg–MT complex,[5,21-24] however, necessitated a more thorough analysis of the stoichiometry of the Hg–MT interaction reported herein since, in our hands[25] and others,[26] the duplication of the published procedures did not give rise to a detectable ^{199}Hg NMR signal. One possible explanation for the failure to observe a ^{199}Hg NMR signal could be related to the preference of mercury(II) for linear 2-coordinate complex formation with thiolate ligands,[27] an example of which has been shown in the crystal structure of the 2:1 complex of cysteine with mercury(II),[28] and the facile interchange that could then occur between this coordination and that of the tetrathiolate-coordinated Hg(II) ion.[5] Another noteworthy property of mercury(II) complexes is their tendency toward more rapid exchange than similar cadmium(II) complexes.[29] This property together with the propensity of Hg(II) for both tetrahedral and linear coordination geometry and the large NMR chemical shift range makes ^{199}Hg NMR spectroscopy more susceptible than ^{113}Cd NMR spectroscopy to problems associated with chemical exchange broadening that can frequently be a major deterrent in metal NMR studies. Therefore, before attempting an extensive structural characterization of the mercury(II) derivative of the protein with ^{199}Hg and ^{199}Hg–^1H NMR techniques, it was necessary to first carry out the studies reported herein to determine to what extent the tetrahedral geometry found with the cadmium(II) derivatives is retained in the mercury(II) derivative of MT. In the course of this study, we provide evidence that indicates that mercury(II) adopts both a tetrahedral and a linear coordination geometry in this protein. Additionally, we have characterized a facile interchange reaction of cadmium(II) and mercury(II) upon mixing the all cadmium(II) and all mercury(II) forms of MT, resulting in a stable mixed-metal species.

Experimental Section

Protein Preparation. Metallothionein was isolated from the livers of rabbits injected subcutaneously seven times on alternate days with 2 mg/kg of $CdCl_2$ (the first and second injections were one-third and two-thirds, respectively, of the full dose). The protein was extracted from these livers by following the method of Winge.[30] After the acetone precipitation, the protein was purified first by gel filtration on Sephadex G-75 and then the isoforms were separated by ion-exchange chromatography. The ion exchange was performed on DEAE Sephacel with a gradient from 0.01 to 0.20 M Tris–Cl at pH 9.0. All experiments described here were done with MT-II. Purity was established with gel electrophoresis on nondenaturing discontinuous gels. HPLC profiles of the MT-II on a TSK G2000 gel filtration column (see below) showed the concentration of dimer and higher aggregates to be less than 10%. Purified protein was concentrated by ultrafiltration, dialyzed against 0.5 mM potassium phosphate buffer at pH 7.5, and stored at −20 °C after lyophilization. Apometallothionein was formed by reducing the pH of the protein solution to 1.5 with HCl.

Metal-Exchange Procedures. Metal-exchange experiments were done in a buffer containing 0.01 M potassium phosphate and 0.15 M KCl. The pH was 6.0 in order to prevent precipitation of the metal hydroxides. The concentration of Cd_7–MT for the mercury(II) titration was 16.4 uM in a 1 mL volume. Aliquots of $HgCl_2$ (from atomic absorption standard, Fisher Scientific) were added, and the solution was allowed to stand for 30 min. A 1-mL aliquot of a slurry (1 g/10 mL) of Chelex 100 was added to the solution to remove displaced cadmium(II) and adventitiously bound mercury(II). Control experiments demonstrated that this treatment does not remove cadmium(II) from the Cd_7–protein. The solution was separated from the Chelex by sedimentation or filtration.

Cadmium(II) concentrations were measured by flame atomic absorption spectroscopy on an IL 157 AA spectrophotometer. Mercury concentrations were measured with the same instrument with use of the Model 555 controlled-temperature furnace. Samples for the mercury determination were diluted in a solution of 5% nitric acid and 0.1% potassium dichromate according to the protocol recommended by the instrument manufacturer. The presence of phosphate was observed to depress the readings obtained for mercury in the atomic absorption spectrophotometer. Accordingly, all samples and standards were made to contain the same buffer concentration at the final dilution. Protein concentrations were determined by measuring the optical absorbance at 220 nm (ϵ = 47 300[31]) after displacement of cadmium(II) by reducing the sample pH to 1.5 with HCl.

The determination of the state of aggregation and alterations in MT shape were done with gel filtration HPLC using a 7.5 mm × 600 mm TSK G2000 column on a Rainin HPLC system. Flow rate was 0.9 mL/min.

Kinetic measurements of the mercury–cadmium interchange reaction were done by recording the OD_{300} on a Gilford 252 spectrophotometer connected to a strip-chart recorder. The temperature was regulated at 20 °C. The kinetic profiles were digitized with a modified "Mouse" interfaced to an IBM PC AT microcomputer. Initial rates of reaction were determined by linear regression of the absorbance data. The integrated rate equation for a bimolecular reaction was fit to the data with a nonlinear, least-squares program that used a modified Gauss–Newton algorithm.[32] UV absorption spectra of the MT solutions and of the $Hg(cys)_2$ complex, which was prepared by stoichiometric metal ion addition, were recorded on Cary 118 spectrophotometer.

UV Spectral Analysis. It was of interest to determine the number of spectrally distinct components that were present during the titration of cadmium(II) metallothionein with mercury(II) since this provided an estimate of the minimum number of unique metal–protein complexes formed. This information can best be extracted from the experimental data by the singular value decomposition (SVD) of the ($m \times n$) matrix of UV spectral data.[33-35] Each of the n columns of this data matrix, **D**,

(10) Zelazowski, A. J.; Piotrowski, J. K. *Biochem. Biophys. Acta* **1980**, *625*, 89–99.
(11) Gerson, R. J.; Shaikh, Z. A. *Biochem. J.* **1982**, *208*, 465–472.
(12) Szymanska, J. A.; Zelazowski, A. J.; Stillman, M. J. *Biochem. Biophys. Res. Commun.* **1983**, *115*, 167–173.
(13) Evans, R. M.; Patieno, S. R.; Wang, D. S.; Cantoni, O.; Costa, M. *Mol. Pharmacol.* **1983**, *24*, 77–83.
(14) Planas Bohne, F.; Taylor, D. M.; Walser, R. *Arch. Toxicol.* **1985**, *56*, 242–246.
(15) Bracken, W. M.; Sharma, R. P.; Bourcier, D. R. *J. Toxicol. Environ. Health* **1984**, *13*, 865–877.
(16) Day, F. A.; Funk, A. E.; Brady, F. O. *Chem. Biol. Interact.* **1984**, *50*, 159–174.
(17) Durnam, D. M.; Palmiter, R. D. *J. Biol. Chem.* **1981**, *256*, 5712–5716.
(18) Samji, S.; Kuliszewski, M. J.; Girgis, G. R.; Nichols, D. M. *Can. J. Bioch. Cell Biol.* **1985**, *63*, 913–918.
(19) Sudmeier, J. L.; Perkins, T. G. *J. Am. Chem. Soc.* **1977**, *99*, 7732–7733.
(20) Vidusek, D. A.; Roberts, M. F.; Bodenhausen, G. *J. Am. Chem. Soc.* **1982**, *104*, 5452–5456.
(21) Sokolowski, G.; Weser, U. *Hoppe*-Seyler's *Z. Physiol. Chem.* **1975**, *356*, 1715–1726.
(22) Holt, D.; Magos, L.; Webb, M. *Chem. Biol. Interact.* **1980**, *32*, 125–135.
(23) Szymanska, J. A.; Law, A. Y. C.; Zelazowski, A. J.; Stillman, M. J. *Inorg. Chim. Acta* **1983**, *79*, 123–124.
(24) Stillman, M. J.; Law, A. Y. C.; Szymanska, J. A. *Chem. Toxicol. Clin. Chem. Met., Proc. Int. Conf.* **1983**, *2nd*, 271–274.
(25) Johnson, B. A.; Armitage, I. M., unpublished observations.
(26) Dean, P. A. W.; Law, A. Y. C.; Szymanska, J. A.; Stillman, M. J. *Inorg. Chim. Acta* **1983**, *78*, 275–279.
(27) Huheey, J. E. *Inorganic Chemistry*; Harper and Row: New York, 1983, pp 465–467.
(28) Taylor, N. J.; Carty, A. J. *J. Am. Chem. Soc.* **1977**, *99*, 6143–6145.
(29) Margerum, D. W.; Cayley, G. R.; Weatherburn, D. C.; Pagenkopf, G. K. In *Coordination Chemistry*; Martell, A. E., Ed.; ACS Monograph 174; American Chemical Society: Washington, DC, 1978; Vol. 2, pp 1–220.
(30) Winge, D. R.; Geller, B. L.; Garvey, J. *Arch. Biochem. Biophys.* **1981**, *208*, 160–166.
(31) Buhler, R. H. O.; Kägi, J. H. R. In *Metallothionein, Proceedings of the First International Meeting on Metallothionein and other Low Molecular Weight Metal-Binding Proteins*; Kägi, J. H. R., Nordberg, M., Eds; Birkhäuser: Basel, Switzerland, 1979; pp 211–220.
(32) Johnson, M. L.; Correia, J. J.; Yphantis, D. A.; Halvorsen, H. R. *Biophys. J.* **1981**, *36*, 575–588.
(33) Forsythe, G. E.; Malcolm, M. A., Moler, C. B. *Computer Methods for Mathematical Computations*; Prentice-Hall: Englewood Cliffs, NJ, 1977; pp 192–239.

consists of a spectrum of MT measured at m wavelengths during the titration with mercury(II). The spectrum of apometallothionein was subtracted from each spectrum so that the resulting spectra represent only the contribution to the UV absorption from the metal–cysteine interaction. In making this correction, it was assumed that the contribution to the UV spectrum by the peptide backbone was unchanged by different coordinating metals,[36] and furthermore, since MT lacks any aromatic amino acids, this correction only affects the spectrum below a wavelength of approximately 250 nm. The number of spectrally unique components corresponds to the number of linearly independent column vectors, that is, to the rank, r, of the matrix. The rank and the r basis spectra from which the data can be reconstructed can be determined with the method of singular value decomposition as follows. The matrix **D** is decomposed into three orthogonal matrices such that $\mathbf{D} = \mathbf{USV}^T$. In this representation, **S** is a diagonal matrix whose elements, the singular values, are ordered by descending value. In the noise-free case, the number of nonzero singular values is the rank of the matrix. In experimental measurements where noise is present, there may be $n - r$ nonzero singular values that represent the noise contribution to the matrix. The r columns of **U** corresponding to nonnoise singular values represent the basis spectra. The corresponding rows of the matrix $\mathbf{V}^T$ represent the titration curve for each spectrum. If the original matrix **D** is represented in this way, it follows that the magnitude of the singular value gives the weight that each basis spectrum contributes to the original data matrix. The criteria used to determine the number of spectral components are described in the Results section of this paper.

The basis spectra determined from the columns of **U** do not, unfortunately, correspond to the spectra of the individual components appearing in the titration.[35] Rather, the component spectra **C**, are a linear combination of the basis spectra, $\mathbf{C} = \mathbf{USB}$, where **B** is a matrix that transforms the basis spectra to the component spectra. The inverse of **B**, $\mathbf{B}^{-1}$, transforms $\mathbf{V}^T$ into a matrix **F** ($= \mathbf{B}^{-1}\mathbf{V}^T$), that represents the titration profiles of each component spectrum in **C**, such that $\mathbf{D} = \mathbf{CF}$. Our method for determining the matrices **C** and **F** is similar to that used by Gemperline[37] in his analysis of liquid chromatography/ultraviolet data. In order to accommodate the constraints described below, we used a nonlinear minimization with a downhill simplex routine.[38] The unknown elements of **B** and **F** were iteratively changed until the difference between the product **BF** and $\mathbf{V}^T$ was minimized. In order for convergence to be obtained, this minimization must be constrained according to several physically meaningful criteria. (1) The first spectra of the series (before the addition of any mercury(II)) represents a single spectral component characteristic of the tetrahedral Cd–S complex present in the native protein. This constraint provides the values for the first column of **B** and the first column of **F**. (2) The cadmium(II) is present in only one spectrally distinct species (the tetrahedral Cd–S complex, see below) throughout the titration. Thus, the first row of **F** is just the measured fractional amount of cadmium(II) present in the MT at each point in the titration. (3) The sum of the number of tetrahedral cadmium(II) and mercury(II) sites cannot exceed seven, the *known* total number of tetrahedral sites in the protein.[2,8] (4) The number of linear mercury(II) sites cannot exceed three times the number of vacant tetrahedral sites. The value of three is somewhat arbitrary. This constraint prevents the existence of linear sites in the protein when it is fully occupied with tetrahedrally coordinated cadmium(II) and mercury(II). (5) The site occupancies cannot be negative. Successful convergence to the same result was obtained by using different initial guesses for the unknown elements of the two matrices.

The spectral analysis was done with Fortran programs on a Vax 11/750 minicomputer. The singular value decomposition used the double-precision subroutine from the Linpack library.[39]

Results

The propensity of excess metal ions to induce aggregation of some proteins necessitated that this be assayed for at the outset of these mercury(II) titration studies. To assay for aggregation we used high-performance liquid chromatography with a size-exclusion column. From the HPLC elution profiles of the MT at several Hg(II):MT stoichiometries, we found no evidence of any significant aggregation induced by the mercury(II) treatment. Evidence for a change in shape was observed by this method, however, which was perhaps not unexpected in view of the change in mercury(II) coordination geometry described below. A similar change in the shape of the Hg(II) derivative of MT has been previously noted.[10,22,24] Figure 1 shows the partition coefficient of the MT on the size-exclusion column at several stages in the mercury(II) titration as a function of salt concentration. The addition of mercury(II) to the Cd_7–MT metallothionein resulted in a progressive increase in partition coefficient at all salt concentrations. This corresponds to a decrease in the Stokes radius relative to that of Cd_7–MT.

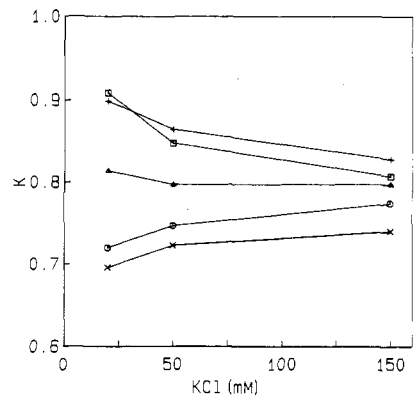

Figure 1. Partition coefficients of metallothionein on a HPLC size exclusion column. The metallothionein was first reacted with 0 (×), 3 (○), 6 (△), 11 (□), or 14 (+) mol equiv of mercury(II).

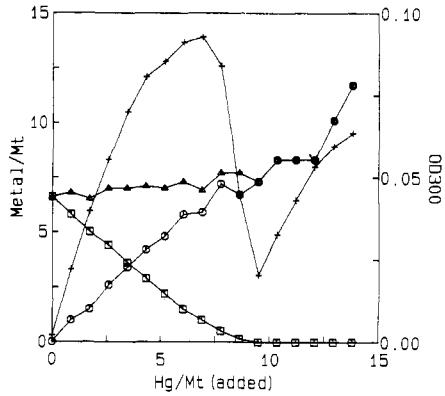

Figure 2. Titration of CD_7–MT with $HgCl_2$. Separate samples of MT were exposed to a series of $HgCl_2$ concentrations, and then treated with Chelex-100 to bind displaced metals. The cadmium (□), mercury (○) and Hg + Cd (△) measured in the protein are illustrated. The OD_{300}'s (+) from the data of Figure 3 are also illustrated.

The stoichiometry of cadmium(II) displacement by mercury(II) was monitored by measuring both the cadmium(II) and mercury(II) remaining in the sample following additions of increasing amounts of mercury(II) to separate samples of the Cd_7–MT and treatment with Chelex as described in the Experimental Section. As illustrated in Figure 2, addition of mercury(II) led to an approximate 1:1 displacement of cadmium(II) from the Cd_7–MT up to approximately 6 equiv of mercury(II). Complete displacement of the cadmium(II) ions from Cd_7–MT occurs upon the addition of 8 equiv of mercury(II). This nearly 1:1 displacement of cadmium(II) is also reflected in the near constancy of total metal ions bound throughout this range (Figure 1). Additional mercury(II) ions continued to be bound after all cadmium(II) ions were displaced. Figure 2 also shows the absorption at 300 nm throughout the titration. For up to 7 mol equiv of added mercury(II), there is an increase in the absorption at 300 nm. Unlike the linear increase in mercury(II) bound to the protein during this part of the titration, the increase in OD_{300} clearly shows a decreasing slope, particularly above a stoichiometry

(34) Yamaoka, K.; Matsuda, T.; Takatsuki, M. *Bull. Chem. Soc. Jpn.* **1980**, *53*, 968–974.
(35) Hofrichter, J.; Henry, E. R.; Sommer, J. H.; Deutsch, R.; Ikeda-Saito, M.; Yonetani, T.; Eaton, W. A. *Biochemistry* **1985**, *24*, 2667–2679.
(36) Vasak, M.; Kägi, J. H. R.; Hill, H. A. O. *Biochemistry* **1981**, *20*, 2852–2856.
(37) Gemperline, P. J. *Anal. Chem.* **1986**, *58*, 2656–2663.
(38) Press, W. H.; Flannery, B. P.; Teukolsky, S. A.; Vetterling, W. T. *Numerical Recipes*; Cambridge: New York, 1986; pp 289–293.
(39) Dongarra, J. J.; Bunch, J. R.; Moler, C. B.; Stewart, G. W. *LINPACK User's Guide*; SIAM Publications: Philadelphia, 1979; pp 11.1–11.23.

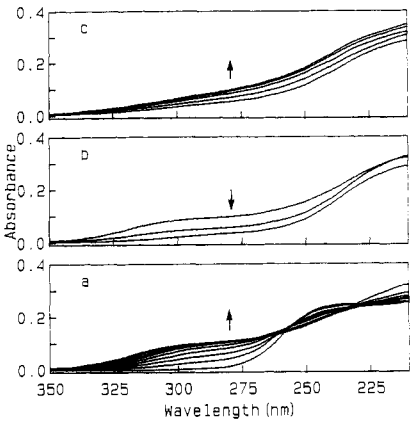

Figure 3. UV spectra of Cd_7–MT during the titration (Figure 2) with $HgCl_2$. The Hg/MT stoichiometry is (a) 0–7, (b) 8–9.5, (c) 10–14. Arrows indicate the direction of increasing mercury(II).

Table I. Singular Values, Autocorrelation of the Columns of the Matrix U, and the Rms Difference between the Original Data Matrix and That Calculated from the Indicated Number of Columns of the Matrices U and V

column no.	SVD	ACU	rms
1	5.0144	0.97	0.0189
2	0.4911	1.00	0.0126
3	0.4286	0.96	0.0026
4	0.0730	0.98	0.0015
5	0.0452	0.98	0.0008
6	0.0192	0.90	0.0006
7	0.0141	0.82	0.0004
8	0.0092	0.83	0.0003
9	0.0066	0.74	0.0002
10	0.0053	0.63	0.0002
11	0.0039	0.80	0.0001
12	0.0036	0.77	0.0001
13	0.0029	0.73	0.0001
14	0.0021	0.53	0.0001
15	0.0017	0.73	0.0000
16	0.0016	0.73	0.0000
17	0.0014	0.61	0.0000

of three to four bound mercury(II) ions. For from 7 to 10 mol equiv of mercury(II) per metallothionein, the OD_{300} drops, and then, above 10 mol equiv, the OD_{300} again increases.

Ultraviolet absorption spectra of the metallothionein following mercury(II) addition and Chelex treatment are shown in Figure 3. As previously noted under somewhat different conditions,[23,24] the spectral changes are complex, showing a multiphasic response at most wavelengths. The spectra with up to four mercury(II) atoms bound per mole of MT show an isosbestic point at 256 nm. No clear isosbestic point is observed above that stoichiometry. It was of interest, therefore, to determine the number of spectrally distinct components taking part in the overall titration. For this purpose, the method of singular value decomposition was applied as described in the experimental section. Table I lists the magnitude of the singular values, the autocorrelation of the columns of U, and the rms difference between the raw data matrix and that reconstructed from the listed number of columns U and V. It can be seen from this table that, when one moves in order of increasing singular value, the first large jump occurs between the fourth and third values. The fact that the columns of U corresponding to these three singular values all have autocorrelations greater than 0.97 supports their assignment as signal rather than noise. Furthermore, a noticeable improvement in rms deviation occurs upon inclusion of each of the first three columns, while the addition of the fourth yields a negligible improvement. The fourth and fifth columns of U show high autocorrelations, suggesting that they are not noise related. Their low singular values and the small improvement in the rms deviation obtained upon their inclusion, however, indicates that their contribution is negligible. The conclusion from this analysis is that only the first three columns of U and V, which correspond to the largest singular

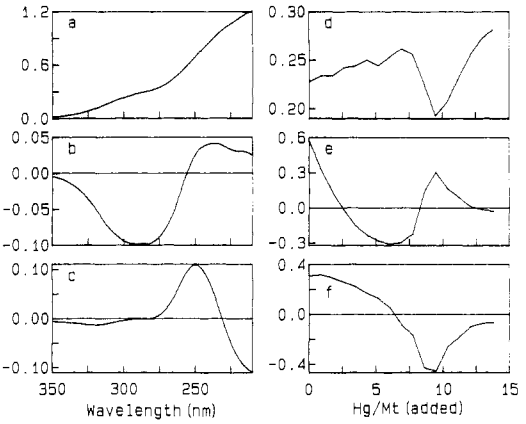

Figure 4. Results of the SVD analysis of the UV spectra (Figure 3) of Cd_7–MT during a titration with $HgCl_2$. Panels a–c illustrate the basis spectra. These are the columns of matrix U that correspond to the largest three singular values. Each column is multiplied by its singular value. Panels d–f illustrate the corresponding columns of the matrix V. These give the amplitudes of the corresponding basis spectra throughout the titration.

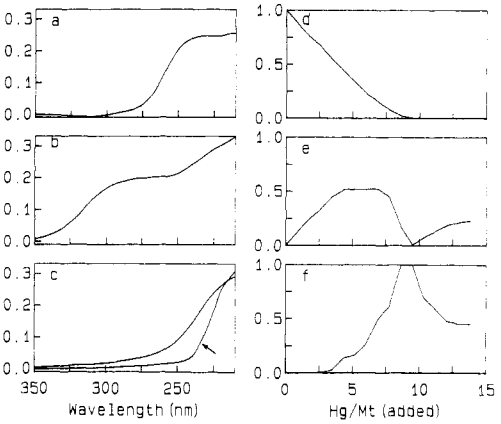

Figure 5. Results of the transformation of the basis spectra of Figure 4 as described in the text. Panels a–c illustrate these spectra, which are a linear combination of the basis spectra of Figure 4. These give the spectral contribution of the three components present during the titration of Cd_7–MT with $HgCl_2$. The spectrum of $Hg(cys)_2$ is indicated in panel c with an arrow. Panels d–f give the fractional abundance of each of these three components during the titration.

values, are required to obtain an excellent description of the data set. This therefore suggests the involvement of three spectrally distinct components in the titration.

The columns of U corresponding to the first three singular values are illustrated in Figure 4. The columns of U have been multiplied by their corresponding singular value. While the orthogonality condition of the SVD technique precludes these spectra from corresponding to physically meaningful spectra, some significance can be ascribed to their appearance. The first (Figure 4a) represents the general trend seen in all the spectra, which is a gradual increase in absorbance toward the high-energy end of the spectrum. The second (Figure 4b), provides a contribution in the 300-nm region of the spectrum, corresponding to tetrahedral Hg–S absorption (see below). The third (Figure 4c), provides a contribution in the 250-nm region, corresponding to the tetrahedral Cd–S absorption (see below). The columns of V (rows of V^T) corresponding to the three largest singular values are also illustrated in Figure 4 (parts d–f). These indicate the fractional contribution of the corresponding basis spectrum (column of U) throughout the titration.

The actual absorption spectra of the individual metal ligand complexes present in the titration are linear combinations of the basis spectra just described. The transformation matrix, **B**, was determined as described in the Experimental Section. The resulting spectra, corresponding to columns of the matrix **C** (=**USB**) are illustrated in Figure 5. The first (Figure 5a), of course,

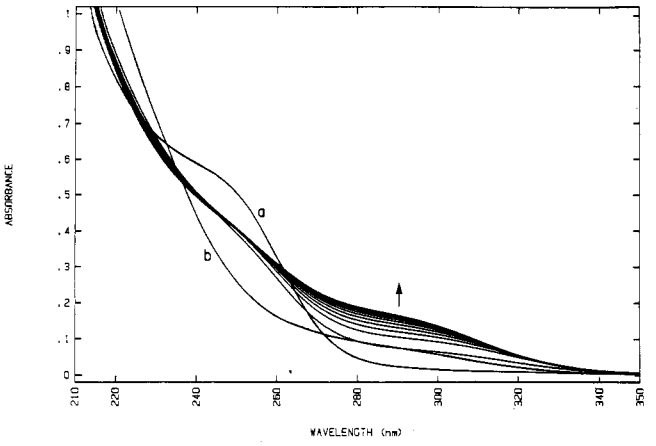

Figure 6. Representative illustration of the time course of spectral changes occurring following the mixing of Cd–MT and Hg–MT. Spectra were collected at 2-min intervals in a Hewlett-Packard diode array spectrophotometer. Spectrum a is that of the all-Cd metallothionein, and spectrum b is that of the all-Hg metallothionein.

corresponds to the first spectrum in the titration. The third component spectrum (Figure 5c) is essentially the same as the spectrum present at the addition of the ninth or tenth equivalent of mercury(II), where there is a negligible contribution from the first two spectra. The second spectrum (Figure 5b), on the otherhand, corresponds to a single component that is never present in more than 60% abundance at any stage in the titration. Figure 5 also shows the titration profiles for each of the three component spectra. The profile for the first component (Figure 5d) is just that corresponding to the observed decrease in cadmium(II) concentration during the titration. The second component (Figure 5e) first rises in abundance as mercury(II) is added to the protein, reaching a plateau in the range from 4 to 7 equiv of added mercury(II), and then declines to a minimum at the ninth equivalent. The third component (Figure 5f) rises in abundance through the titration, reaching a maximum when the first and second components are zero at 9 equiv of added mercury(II) and then subsequently declines.

In these studies of mercury(II) derivatives of MT, it was also of interest to determine whether interprotein exchange of metals occurs with the cadmium(II) form of MT as has been recently demonstrated to occur between Cd and Zn–MT.[40] In order to address this issue, we made use of the fact that the OD_{300} is near a minimum at the point where all the cadmium(II) has been displaced by mercury(II) (Figure 2) and that the Cd_7–MT has no absorbance at 300 nm. Thus, a nonreacting mixture with equal concentrations of the two species should show an absorbance approximately half that of the OD_{300} of the mercury(II)-containing MT. On the other hand, if the proteins exchange metals and form the mixed Cd–Hg protein, it can be seen from Figure 2 that an increase in absorbance at 300 nm will result. When the two proteins were mixed, it was observed that the initial OD_{300} was intermediate between the two forms, but with time increased to values that were characteristic of the mixed-metal (Cd, Hg) MTs. One example of this interchange is illustrated in Figure 6. For quantitative analysis of the interchange, the change in OD_{300} was followed with time at six protein concentrations. A plot of the initial rate of absorbance change vs. the square of the protein concentration was linear, supporting a bimolecular reaction mechanism. The rate constant was calculated by simultaneously fitting the OD_{300} from all six reactions to eq 1

$$OD_{300} = f[P]_i\epsilon_{Cd} + f[P]_i\epsilon_{Hg} + (1 - f)[P]_i\epsilon_{Hg,Cd} \qquad (1)$$

where

$$f = \frac{1}{1 + k[P]_i t}$$

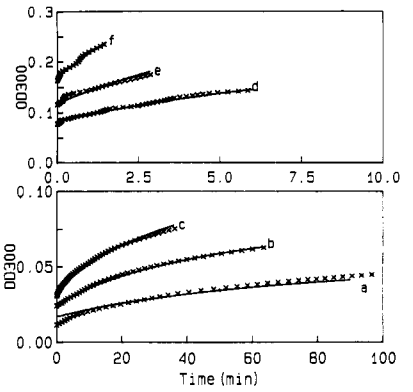

Figure 7. Time course of the OD_{300} during the reaction of Cd–MT and Hg–MT. The initial concentrations of the two proteins are (a) 1.0, (b) 1.5, (c) 2.0, (d) 5.1, (e) 7.1, and (f) 10.1 μM. The crosses give the measured data. The solid lines are calculated from the best-fit parameters of eq 1, when simultaneously fit to all six data sets.

and $[P]_i$ is the initial concentration of the cadmium(II) metallothionein, the ϵ's are the extinction coefficients at 300 nm for the all-cadmium, all-mercury, and mixed-cadmium–mercury metallothioneins, t is the time, and k is the rate constant for the bimolecular reaction. Only the first 20% of each reaction was fitted, as once significant metal exchange has occurred, the kinetics are likely to be more complex. Figure 7 shows the experimental data and the fitted curve. The square root of the variance of the fit was 0.003 absorbance units, indicating an excellent fit to the data. The calculated rate constant is 182 M^{-1} s^{-1} (65% confidence interval, 152–214).

Discussion

Numerous studies now demonstrate that mammalian metallothioneins are inducible by mercury, as well as by zinc, cadmium, and copper. Very little was known, however, about either the structure of the resulting Hg–MT or the Hg–MT exchange properties. Our results, demonstrating quantitative displacement of cadmium(II) by mercury(II), are consistent with earlier reports of mercury(II) interaction with metallothionein[22,23,36,41,42] and with known affinities of these metals for thiolate ligands. Together, these results suggest that, in vivo, in the absence of competition of other sites for mercury(II) (which may be important), intracellular mercury(II) will displace cadmium(II) and by inference zinc(II) bound to metallothioneins.

Previous investigations of the shape of mammalian metallothioneins demonstrated by size-exclusion chromatography that MT behaved as a prolate ellipsoid with an axial ratio of about 6.[43] The recent analysis of the X-ray crystal structure confirms that the protein has a nonspherical shape, but gives a smaller axial ratio of 3.[8] Vasak et al.[44] noted that the Stokes radius of the cadmium(II) and zinc(II) MTs, as determined by size-exclusion chromatography, are dependent on the ionic strength of the buffer. These investigators suggested that the smaller Stokes radius observed at higher ionic strengths results from a minimization of charge repulsion between the two metal clusters. While we have not explicitly calculated the Stokes radius, our size-exclusion HPLC results on Cd–MT confirm the decreased radius at higher ionic strengths. More pertinent to the current study is the observation that at all ionic strengths studied, the mercury(II)-containing MT shows a greater partition coefficient than does the Cd_7–MT. This result is consistent with a decreased Stokes radius of the protein after even partial displacement of cadmium(II) by mercury(II). Such a difference is Stokes radius has also been observed between the cadmium and copper forms of mammalian MTs.[45]

(40) Nettesheim, D. G.; Engeseth, H. R.; Otvos, J. D. *Biochemistry* **1985**, *24*, 6744–6751.
(41) Sokolowski, G.; Pilz, W.; Weser, U. *FEBS Lett.* **1974**, *48*, 222–225.
(42) Nielsen, K. B.; Atkin, C. L.; Winge, D. R. *J. Biol. Chem.* **1985**, *260*, 5342–5350.
(43) Kägi, J. H. R.; Himmelhoch, S. R.; Whanger, P. D.; Bethune, J. L.; Vallee, B. L. *J. Biol. Chem.* **1974**, *249*, 3537–3542.
(44) Vasak, M.; Berger, C.; Kägi, J. H. R. *FEBS Lett.* **1984**, *168*, 174–178.

Optical absorption studies can be used to obtain insight into the nature of the metal–ligand coordination in metallothioneins. Vasak et al.[36] have used Jørgensens optical electronegativity theory to assign the UV absorption due to metals in zinc(II), cadmium(II), and mercury(II) metallothioneins as ligand–metal charge-transfer bands (LMCT). The positions of the lowest energy bands observed in the spectra are consistent with the known electrooptical properties of the ligands and metals involved. In particular, a Cd–S transition is expected at approximately 250 nm and the Hg–S transition is expected at lower energy (ca. 300 nm). These Cd–S and Hg–S ligand–metal charge-transfer bands have also been assigned to tetrahedral coordination sites in other proteins.[46,47]

Earlier reports of the analysis of the metal–ligand interactions that contribute to the UV spectra of MTs have not dealt with the problem of separating out the multiple components that can be present in these spectra. The SVD analysis indicates at least three spectrally distinct components take part in the titration of Cd_7–MT with mercury(II). The first, of course, corresponds to the tetrahedral Cd–S LMCT bands assigned by Vasak et al.[36] The second component, which is not present in pure form at any point in the titration and is only extractable with a spectral deconvolution method such as the SVD analysis, corresponds to tetrahedral Hg–S LMCT bands as assigned by Vasak et al.[36] The third component shows a spectrum which is characteristic of that expected for a linear Hg–S complex[48] (Figure 5c).

Earlier investigators have suggested that the displacement of cadmium(II) by mercury(II) occurs with retention of the tetrahedral coordination geometry.[36] However, Sokoloski et al.[41] in their studies on a Hg^{II}_8–MT by X-ray photoelectron spectroscopy suggested that an uncharacterized but dramatic alteration in structure occurs upon mercury(II) binding. The nearly 1:1 displacement of cadmium(II) by mercury(II) we observed with up to 6 equiv of added mercury(II) is consistent with a replacement of cadmium by mercury(II) with retention of tetrahedral geometry. However, the reduced displacement ratio seen above a mercury(II) stoichiometry of approximately 6 and, more importantly, the results of the SVD analysis of the UV spectra, are consistent with a shift to a different coordination geometry before all the cadmium(II) is displaced. This is shown most clearly in Figure 5e where it can be seen that approximately the first four mercury(II) ions displace the cadmium(II) ions with retention of the tetrahedral geometry. Above this stoichiometry, the spectral data are consistent with a linear geometry for the additional mercury(II) ions. This is demonstrated by the similarity to the spectrum of $Hg(cys)_2$, which is known to be linear from the crystal structure[28] (Figure 5C) and is consistent with the known preference of mercury(II) for linear two-coordinate complexes. It is quite possible that the shift in coordination geometry at this point in the titration may be correlated with a difference in coordination geometry between the four and three metal clusters in MT. Above a mercury(II)/MT stoichiometry of 7 there is a precipitous drop in the occupancy of the tetrahedral geometry. The peak occupancy of the linear form is observed at a mercury(II)/MT stoichiometry of 9. The nearly 2:1 cysteine:mercury(II) ratio at this point is also consistent with this assignment to the linear coordination geometry. Above a mercury(II)/MT stoichiometry of 10, the analysis suggests that a mixture of the linear and tetrahedral coordination geometries are present. At these Hg/protein stoichiometries, the natural metal-binding capacity of the protein has almost certainly been exceeded, and consequently our results are most relevant at levels below this.

Insofar as MT is involved in the buffering of essential metal ions such as copper and zinc and with the sequestration of toxic metals such as mercury and cadmium, the process of the exchange of metals on and off the protein is crucial to its in vivo function. If cadmium(II) displacement by mercury(II) is a simple competition for free sites, the exchange should be limited by the off rate of cadmium(II) from the MT. A rough calculation of this rate can be made by using a value of $K = 10^{15}$ M^{-1} for the association constant[2] and assuming that the on rate is diffusion-controlled (ca. 10^{10}). The off rate calculated in this way is on the order of 10^{-5} s^{-1}. This extremely low rate should limit the replacement reaction time scale to days. Instead, preliminary kinetic measurements suggest time scales on the order of a minute or less. Clearly the mercury(II) must "facilitate" the displacement reaction, presumably by a mechanism such as a concerted reaction with a trivalent sulfur intermediate.

The displacement of cadmium(II) by mercury(II) indicates that the affinity for mercury(II) is higher. The published value[49] for the $Hg(cys)_2$ affinity constant is 10^{44} M^{-2}. Given the very low off rates expected, therefore, for cadmium(II) and especially for mercury(II), the apparent exchange of these metals between the two forms of the protein is surprising. Both forms of the protein were pretreated with Chelex-100; hence, the free metal concentration should be negligible. A consideration of the expected off rates for the metals and of the bimolecular reaction rate observed suggests that a direct interaction between Cd–MT and Hg–MT is responsible for the metal exchange. Direct interaction between MT and other metalloproteins during metal exchange has also been suggested by other investigators.[50] Consideration of the crystal structure of the protein[8] shows that unlike many metalloproteins, the metal sites are not buried deeply within the protein. The high metal and cysteine contents found in MT effectively preclude the burial of the metal sites, rendering them available to interact with other proteins. This presumably is crucial to the in vivo function of this protein. The thiolate ligands and chelate effect of the protein ensure a high affinity for toxic metals, while the ligand availability may lower kinetic barriers to the exchange of essential metals to other proteins during biosynthesis.

Conclusions

The above results documenting the presence of different mercury(II)–ligand geometries in MT, along with the known lability of mercury complexes as observed by ^{199}Hg NMR,[51] emphasize the difficulties present in obtaining structural information from ^{199}Hg NMR spectra of MTs. If the exchange of individual mercury(II) ions between the two geometries is facile, chemical exchange broadening could readily render the resonances unobservable. On the basis of this new understanding of how the occupancy of the different forms change through the titration, however, we are currently initiating new efforts to observe ^{199}Hg NMR signals from MT. We would also like to emphasize the power of the singular value decomposition technique in analyzing spectral data. This technique has not received wide recognition yet it is potentially applicable in a wide variety of spectroscopic studies.

Acknowledgment. This work was supported by Grant No. DK 18778 from the National Institutes of Health. We wish to thank Drs. Joseph and Celia Bonaventura for allowing us to use their HP diode array spectrophotometer.

Registry No. Hg^{2+}, 14302-87-5; Cd, 7440-43-9.

(45) Winge, D. R.; Miklossy, K.-A. *Arch. Biochem. Biophys.* **1982**, *214*, 80–88.
(46) Beltramini, M.; Lerch, K.; Vasak, M. *Biochemistry*, **1984**, *23*, 3422–3427.
(47) Tamilarasn, R.; McMillin, D. R. *Inorg. Chem.* **1986**, *25*, 2037–2040.
(48) Steinberg, I. Z.; Sperling, R. In *Conformation of Biopolymers*; Ramachandran, G. N., Ed.; Academic: London, 1967; pp 215–233.
(49) Stricks, W.; Kolthoff, I. M. *J. Am. Chem. Soc.* **1953**, *75*, 5673–5681.
(50) Li, T.-Y.; Kraker, A. J.; Shaw, C. F.; Petering, D. H. *Proc. Natl. Acad. Sci. U.S.A.* **1980**, 6334–6338.
(51) Carson, G. K.; Dean, P. A. W. *Inorg. Chim. Acta* **1982**, *66*, 157–161.